Published in final edited form as:
Lab Chip. 2014 March 7; 14(5): 972–978. doi:10.1039/c3lc50959a.

On-demand, competing gradient arrays for neutrophil chemotaxis†

Hansang Cho[#], **Bashar Hamza**[#], **Elisabeth A. Wong**, and **Daniel Irimia**[*]
BioMEMS Resource Center, Massachusetts General Hospital, Harvard Medical School, and Shriners Hospital for Children, Charlestown, MA, 02129, USA.

[#] These authors contributed equally to this work.

Abstract

Neutrophils are the most abundant type of white blood cells in the circulation, protecting the body against pathogens and responding early to inflammation. Although we understand how neutrophils respond to individual stimuli, we know less about how they prioritize between competing signals or respond to combinational signals. This situation is due in part to the lack of adequate experimental systems to provide signals in controlled spatial and temporal fashion. To address these limitations, we designed a platform for generating on-demand, competing chemical gradients and for monitoring neutrophil migration. On this platform, we implemented forty-eight assays generating independent gradients and employed synchronized valves to control the timing of these gradients. We observed faster activation of neutrophils in response to fMLP than to LTB_4 and unveiled for the first time a potentiating effect for fMLP during migration towards LTB_4. Our observations, enabled by the new tools, challenge the current paradigm of inhibitory competition between distinct chemoattractant gradients and suggest that human neutrophils are capable of complex integration of chemical signals in their environment.

1. Introduction

Neutrophils are the predominant immune cells in circulation. They protect the body against invading pathogens by migrating from the circulation to tissues, following a hierarchy of chemotactic signals that guide their recruitment to the sites of injury.[1–3] Their ability to prioritize one chemoattractant over another is important to efficiently navigate the complex tissues.[4–6] Particularly, two signalling pathways for neutrophil chemotaxis have been demonstrated that involve phosphatidylinositol-3-OH kinase (PI(3)K) phosphatase and p38 mitogen-activated protein kinase.[7–10] The activation of the PI(3)K pathway is triggered by tissue-derived chemokines, *i.e.* leukotriene B4 (LTB_4) and interleukin 8 (IL8) secreted by endothelial cells, macrophages, and mast cells. The activation of the p38 pathway is triggered by bacteria-derived chemokines, i.e. *N*-formyl-methionyl-leucyl-phenalanine (fMLP) or complement factor 5a (C5a),[8–11] and can override signalling through the PI(3)K pathway.

In the past few years, significant progress has been made towards a better understanding of how neutrophils respond to competing signals.[12–15] However, a precise quantification of the responses to temporal sequences of stimuli has not been studied. This is mainly due to the difficulty of extracting the role of individual chemokines at each stage during an immune

[†]Electronic supplementary information (ESI) available. See DOI: 10.1039/c3lc50959a

[*]*dirimia@hms.harvard.edu*.

system response *in vivo* and the lack of adequate *in vitro* assays capable of providing complex chemoattractant signals in a controlled and temporal fashion. One of the common platforms for studying human leukocytes trafficking *in vitro* is the transwell filter assay that provides an end-point count of migrating cells towards a single chemoattractant.[16] Microfluidic-based platforms, on the other hand, have provided researchers with valuable tools to precisely quantify the full response of leukocytes to stable chemoattractant gradients on a single-cell resolution.[17] The tree-shaped single gradient generator was among the first of these platforms.[18,19] Other microfluidic devices were designed to generate overlapping gradients from multiple sources.[20–22] Pneumatic valves and light-induced methods allowed for the generation of spatiotemporal switchable gradients.[23,24] Simpler platforms also emerged without the need for fluidic pumps.[25–27] Of those, gel-based platforms separated cellular and chemokine compartments,[28,29] surface-tension based platforms were implemented in a dense array format to create a high-throughput chemotaxis assay,[30–32] and a multi-layered platform provided week-long lasting gradients.[33] However, none of the existing platforms can provide spatial-temporal and simultaneous gradients in a large-scale manner for systematic studies of neutrophil chemotaxis extracted from a single experiment and requiring a single blood processing procedure.

Here, we designed a chemotaxis platform capable of exposing neutrophils to 48 unique combinations of dual chemoattractant gradients. We employed the platform to test human neutrophil responses in the presence of simultaneous but spatially opposite chemoattractant gradients. We observed that human neutrophils could prioritize their responses toward fMLP over LTB_4 chemoattractants and found that response time can be accelerated in the presence of chemoattractant combinations. These observations challenge the current paradigm of down-regulating interactions between chemokine signalling pathways.[7] Our observations suggest that in certain situations, synergistic effects are possible between different chemokine gradients, suggesting more sophisticated interplay can be taking place between chemokine signalling pathways in neutrophils.

2. Materials and methods

2.1 Microfluidic platform fabrication

The fabrication was performed using standard soft lithographic techniques on two six-inch wafers (Fig. 1A). Multiple layers of photoresist (SU8, Microchem, Newton, MA, USA) were aligned on the network wafer, with thicknesses of 5 μm for neutrophil migration channels, 10 μm for the entrance zone to the migration channels, 50 μm for sinks and all compartments on the network wafer. A single layer of 50 μm in thickness was patterned for pneumatic chambers on the valve control wafer.

A mixture of PDMS (Polydimethylsiloxane) and its curing agent (SYLGARD 184 A/B, Dow Corning, Midland, MI, USA) at 10:1 was spun to a thickness of 150 μm and baked in an oven set to 65 °C for at least 3 hours. For the control layer, the mixture was poured to a thickness of ~3 mm and cured at room temperature for 48 hours to avoid the shrinkage of PDMS and dimensional mismatch with the network layer (Fig. 1B). Afterwards, the control layer was peeled off and punched with a 1.5 mm puncher (Harris Uni-Core, Ted Pella Inc., Reading, CA, USA) to define two control lines for side and central valves. The network and control layers were then treated with oxygen plasma for bonding. A volume of 1 mL of high purity ethanol (99.9%, Sigma-Aldrich, St. Louis, MO, USA) was gently spread on the top of the network layer to act as a surfactant.[34] The control layer was then placed and aligned to the network layer (Fig. 1C). After removal of excess ethanol by suction, the two aligned layers were transferred back to the oven and left to bake overnight, cut, gently peeled off, and punched with a 1.2 mm puncher. The assembled PDMS layers were treated with oxygen plasma at 50 mW, 10 ccm, for 35 seconds (PX-250, March Plasma Systems, Petersburg, FL,

USA) for irreversible bonding to a glass-bottomed UniWell plate (MGB001-1-2-LG, Matrical Bioscience, Spokane, WA, USA).

To avoid the collapse and permanent bonding of the 'default-closed' valves to the glass substrate, a special protocol was employed during the bonding of the assembled PDMS layers. First, the 'default-closed' side valves were kept elevated off the glass surface in an open position by applying negative pressure around –27 psi during a 15 minute bonding step when the plasma-treated surfaces remained active. Afterwards, the valves were closed and opened fast and repeatedly, to deactivate plasma-activated surfaces by touching and separating them before bonding can occur, and to ensure full functionality of the valves (Fig. 1D). Finally, the platforms were immediately primed for 30 minutes with a solution of human-fibronectin (Sigma-Aldrich), diluted to 100 nM in distilled water that had been autoclaved and filtered (0.2 μm filter, AM9920, Life Technologies, Grand Island, NY, USA). Fibronectin-treated surfaces were then rinsed with sterile water and the platform was filled with cell culture medium (Iscove's Modified Dulbecco's Medium) supplemented with 10% FBS (Sigma-Aldrich) and 1% penicillin/streptomycin (Life Technologies).

2.2 Cell preparation

De-identified, fresh human blood samples from healthy volunteers, aged 18 years and older, were purchased from Research Blood Components (Alston, MA). Peripheral blood was drawn in heparinized-tubes (Vacutainer; Becton Dickinson) and human neutrophils were isolated within 2 hours after blood collection using HetaSep followed by the EasySep Human Neutrophil Enrichment Kits (STEMCELL Technologies, Vancouver, Canada). After isolation, cells were washed using cell culture medium without serum. The cell membrane was stained with red fluorescent dye (PKH26PCL, Sigma-Aldrich). The stained neutrophils were re-suspended in medium at a density of 20×10^6 cells mL^{-1}. Ten μL of cell suspension were injected into the cell compartment and incubated at 37 °C supplied with 5% CO_2 for 30 minutes. Afterwards, 10 μL of each chemokine solution was injected into its designated chemokine compartment.

2.3 Time-lapse imaging

To simultaneously image the moving neutrophils in the arrayed 48 platforms, we used an automated microscope equipped with a motorized stage in the *x* and *y* directions (EclipseTi, Micro Video Instruments, Avon, MA, USA). A perfect focusing system (PFS, Nikon) compensated for any mechanical disturbance in the *z* direction and maintained the quality of focusing through the experiment. For live-cell imaging, we integrated the microscope with a heated incubating stage (LiveCell 05-11-0032 Rev B, Pathology Devices Inc., Westminster, MD, USA), which was set at 37.7 °C, 5% CO_2, and 85% humidity. We imaged the cells every 3 minutes using phase contrast and fluorescence for 2 hours with a 4× objective lens and in a large-area mode of 2×2 mm^2 with a 15% stitching.

2.4 Analysis of cellular motility

Image analysis of the time-lapse movies at each location was performed using the NIS Elements (Nikon Inc., Melville, NY, USA) and automated using the open-sourced software, CellProfiler (Broad Institute, Boston, MA, USA). The analysis was limited to the first hour of experiments, when the slope of chemical gradients maintained about 80% of the initial slope, at the start of the experiments. Also, we restricted the analysis to the neutrophils inside the migration channels and measured migration and neutrophil response time in the *x* direction along the migration channels. We defined the neutrophil "response time" as the time for resting neutrophils to fully attach to the fibronectin-coated glass surface and migrate at least 150 μm (70 μm in the entrance region and 80 μm inside the channel). Raw data was processed and analyzed using MATLAB (MathWorks, Inc, Natick, MA).

3. Results and discussion

3.1 Design of chemotaxis platform providing on-demand, simultaneous gradients, and on-chip validation

To study neutrophil responses to various combinations of gradients in complex immune environments, we designed a microfluidic platform that provides precise spatial and temporal control of chemokine gradients, and confines neutrophils in small channels during chemotaxis. The platform has a cellular compartment in the center (cell, Fig. 2), two chemokine chambers of 50 nL in volume, and two chemokine compartments on the sides (CK1 and CK2, Fig. 2). Two arrays of migration channels ($5 \times 10 \times 500\ \mu m^3$ in height, width, and length) connect the chemokine chambers and the central compartment. The platform contains two types of pneumatic valves to generate two distinct gradients of chemokines and apply these to cells at the same time (Fig. 2A). Two 'default-closed' valves are placed between chemokine compartments and chemokine chambers and are opened temporarily during chemokine priming of the chambers and migration channels (Fig. 2B, D 1–2).[35] One 'default-open' central valve is closed during cell loading and chemokine priming, and when it opens, cells are immediately exposed to gradients and start chemotaxis (Fig. 2C, D 3–4). In order to generate similar gradients of the two chemoattractants having different molecular weights, we designed two sinks between the migration channels and the central compartment to compensate for the difference in diffusivity of the two chemokines during the priming step. These sinks are twenty times larger in volume than the migration channels. For valve operation, a positive pressure (PP), approximately 30 psi relative to ambient pressure, was used to close the 'default-open' valves and a negative pressure (NP), approximately –27 psi, to open 'default-closed' valves. All 48 pairs of valves on the platform are controlled by only two pneumatic lines, enabling the synchronized operation of forty-eight independent platforms.

3.2 Validation of the spatial and temporal chemokine gradients

We visualized the formation of chemical gradients inside the devices using fluorescent dyes. To account for the differences in molecular weight among different chemokines, we tested fluorescein sodium salt (molecular weight 376 Da) and various FITC-conjugated dextrans (between 3 kDa and 70 kDa Fig. 3). The process started with priming the channels by opening the side valves and filling the side compartments and migration channels with chemokine (Fig. 3A). The concentration of FITC-dextran in the chemokine compartment and channels stabilized in between 2 minutes for fluorescein of 376 Da, and 18 minutes for the 70 kDa dextran (Fig. 3B–D). During the priming period, no leakage of fluorescein or fluorescently labelled dextran inside the central compartment was observed. Later, the central valve was opened to form a stable gradient along the channels, between the central and side compartments (Fig. 3E). Gradients of fluorescein and FITC-dextran of 3 kDa stabilized within 3 minutes along the migration channels (Fig. 3F, G) and the central compartment (Fig. 3H). For larger molecular weight dyes (10, 40 and 70 kDa), gradients stabilized within 10 minutes after opening the central valve. The gradients along the migration channels remained at least 80% of their original slope during the first hour. The duration of the stable gradients, validated by dye experiments, provided the effective period of the platform for chemotaxis measurements.

3.3 Quantification of directional migration in response to competing gradients

To probe the response of neutrophils to two simultaneous chemoattractant gradients, we introduced fMLP and LTB_4 to the side compartments and introduced neutrophils to the central compartment. The two chemokines stimulate cell migration through distinct pathways that involve PI(3)K and p38 MAPK, respectively.[7] After opening the central valve, we observed a higher number of neutrophils migrating toward the source of fMLP at

100 nM compared to LTB_4 at 100 nM (Fig. 4A, ESI† movie 1). This bias was consistent with previously reported data[7–10] suggesting a hierarchy in which end-point chemoattractants (fMLP) override intermediate-range chemoattractants (LTB_4). The lower priority towards LTB_4 was evident from the delay to initiate persistent migration when compared to the higher-priority response toward fMLP. For systematic comparison, all conditions were tested in a single run with neutrophils from the same donor and each condition was repeated three times.

The "response time" as defined in this work is different from the "activation time" previously reported[7] in that it includes, in addition to the time for cells to initiate migration along the gradient, the time to fully establish directional migration in migration channels. This definition was used to avoid the noisy and random changes in speed and directionality of neutrophils randomly distributed in the central compartment and take advantage of the consistent measurement inside confined channels.

The response times to the two chemokines were different. It took 27.0 ± 5.3 min to establish fully developed directional migration toward 10 nM fMLP gradient, compared to 34.0 ± 5.7 min toward 100 nM LTB_4 (Fig. 4B). The first neutrophils migrated through the channels and reached the fMLP chamber 36 minutes after the central valve was opened, compared with 51 minutes for the LTB_4. More neutrophils accumulated in the side chambers in response to fMLP compared to LTB_4 and the accumulation continued for more than 2 hours (Fig. 4C).

The migration speed to various concentrations of chemokines, showed similar profiles for fMLP and LTB_4, with a peak speed of 13.6 ± 0.7 $\mu m\ min^{-1}$ at 10 nM of fMLP alone (Fig. 4D), consistent with the average migration speed previously reported in other studies.[10] The response time decreased with increasing concentrations of chemokines, and was systematically shorter for fMLP compared to LTB_4 at similar concentrations (Fig. 4E). These differences in response times cannot be accounted for by the differences in diffusion coefficient between of the two chemokines, which have very similar molecular weights (fMLP: 438 Da and LTB_4: 338 Da). Moreover, the time for either chemokine to cross the central compartment was much shorter than cellular response time. Therefore, the observed differences in response time towards the two chemokines are intrinsic to neutrophils. Additional evidence was provided by imaging the faster attachment of human neutrophils to the glass bottom of the central chamber and polarization in the presence of fMLP compared to LTB_4 (ESI† Fig. S1). Specifically, we observed that neutrophils fully attached to the glass substrate and polarized within 10 minutes after loading in the presence of uniform fMLP at 100 nM. On the other hand, neutrophils did not adhere fully or were still round at 10 minutes in the presence of uniform LTB_4 at 100 nM or no chemokine, respectively. Therefore, faster attachment and polarization are the likely explanations for the shorter response time in the presence of fMLP compared to LTB_4.

The two chemoattractants used in this study, LTB4 and fMLP, have comparable molecular weight with the fluorescein sodium salt used during platform validation. Thus, it is expected for their chemokine gradients to evolve similarly in time with the gradients of fluorescein dye. Considering the reported 20% reduction of the fluorescein gradient within the first hour, we estimate that 80% of original gradients of chemokines are still present at one hour. These gradients were effective for directing neutrophil migration for more than 2 hours after the start of the experiment. Therefore, this platform can potentially be used with chemoattractants of larger molecular weight, and the data from the characterization of the device using larger molecular weight FITC-dextran could serve as a guide for these conditions.

3.4 Real-time evaluation of chemotaxis cross-activation

To investigate the response of neutrophils to stimulation by simultaneous gradients of fMLP and LTB_4, we measured the speed and response time of neutrophils at various concentrations (Fig. 5). Neutrophil migration speed toward fMLP gradients at 10 nM increased by less than 10% in the presence of LTB_4 gradient at 100 nM (from 13.6 ± 0.7 to 15.4 ± 0.7 $\mu m\ min^{-1}$, Fig. 5A). The increase was comparable to that toward the LTB_4 gradient at 100 nM in the presence of the fMLP gradient at 10 nM (from 13.3 ± 0.6 to 14.2 ± 0.6 $\mu m\ min^{-1}$ Fig. 5B). The response time for chemotaxis toward fMLP was shortened by 10% in the presence of the LTB_4 gradient (from 27.0 ± 5.3 to 23.7 ± 0.8 min, Fig. 5C). Significantly shorter response times were observed for chemotaxis toward LTB_4 in the presence of the fMLP gradient (from 34.0 ± 5.7 to 27.0 ± 2.1 min, Fig. 5D). In all of the control conditions, neutrophils did not enter into the migration channels (ESI† Fig. S2).

4. Conclusions

We designed a chemotaxis platform capable of providing up to 48 stable combinations of chemoattractant gradients by the simple operation of two pneumatic lines. We observed a hierarchical neutrophil response to competing gradients and performed precise measurements of the speed and response time. We quantified the dominant effect of the end-point fMLP gradient over an intermediate-range LTB_4 chemoattractant gradient. We observed surprisingly shorter chemotactic response times toward LTB_4 gradients in the presence of fMLP compared to gradients of only LTB_4 or fMLP.

Supplementary Material

Refer to Web version on PubMed Central for supplementary material.

Acknowledgments

This work was supported in part by funding from the National Institutes of Health, grants GM092804, DE019938, and EB002503.

References

1. Liu M, Chen K, Yoshimura T, Liu Y, Gong W, Wang A, Gao J-L, Murphy PM, Wang JM. Sci. Rep. 2012; 2:1–7.
2. Mackay CR. Nat. Immunol. 2001; 2:95–101. [PubMed: 11175800]
3. Nathan C. Nature. 2002; 420:846–852. [PubMed: 12490957]
4. Arner P. J. Intern. Med. 2007; 262:404–407. [PubMed: 17875175]
5. Serhan CN, Yacoubian S, Yang R. Annu. Rev. Pathol.: Mech. Dis. 2008; 3:279–312.
6. McDonald B, Pittman K, Menezes GB, Hirota SA, Slaba I, Waterhouse CCM, Beck PL, Muruve DA, Kubes P. Science. 2010; 330:362–366. [PubMed: 20947763]
7. Heit B, Robbins SM, Downey CM, Guan Z, Colarusso P, Miller BJ, Jirik FR, Kubes P. Nat. Immunol. 2008; 9:743–752. [PubMed: 18536720]
8. Irimia D. Annu. Rev. Biomed. Eng. 2010; 12:259–284. [PubMed: 20450351]
9. Foxman EF, Kunkel EJ, Butcher EC. J. Cell Biol. 1999; 147:577–588. [PubMed: 10545501]
10. Kim D, Haynes CL. Anal. Chem. 2012; 84:6070–6078. [PubMed: 22816782]
11. Heit B, Liu L, Colarusso P, Puri KD, Kubes P. J. Cell Sci. 2008; 121:205–214. [PubMed: 18187452]
12. Foxman EF, Campbell JJ, Butcher EC. J. Cell Biol. 1997; 139:1349–1360. [PubMed: 9382879]
13. Funamoto S, Meili R, Lee S, Parry L, Firtel RA. Cell. 2002; 109:611–623. [PubMed: 12062104]
14. Quinton LJ. Am. J. Physiol. 2004; 286:465L–472.

15. Liu X, Ma B, Malik AB, Tang H, Yang T, Sun B, Wang G, Minshall RD, Li Y, Zhao Y, Ye RD, Xu J. Nat. Immunol. 2012; 13:457–464. [PubMed: 22447027]
16. Boyden S. J. Exp. Med. 1962; 115:453–466. [PubMed: 13872176]
17. Wu J, Wu X, Lin F. Lab Chip. 2013; 13:2484–2499. [PubMed: 23712326]
18. Jeon NL, Dertinger SKW, Chiu DT, Choi IS, Stroock AD, Whitesides GM. Langmuir. 2000; 16:8311–8316.
19. Li Jeon N, Baskaran H, Dertinger SKW, Whitesides GM, Van de Water L, Toner M. Nat. Biotechnol. 2002; 20:826–830. [PubMed: 12091913]
20. Atencia J, Morrow J, Locascio LE. Lab Chip. 2009; 9:2707–2714. [PubMed: 19704987]
21. Choi E, Chang H-K, Young Lim C, Kim T, Park J. Lab Chip. 2012; 12:3968–3975. [PubMed: 22907568]
22. Qasaimeh MA, Gervais T, Juncker D. Nat. Commun. 2011; 2:464. [PubMed: 21897375]
23. Irimia D, Liu S-Y, Tharp WG, Samadani A, Toner M, Poznansky MC. Lab Chip. 2006; 6:191–198. [PubMed: 16450027]
24. Beta C, Wyatt D, Rappel W-J, Bodenschatz E. Anal. Chem. 2007; 79:3940–3944. [PubMed: 17432827]
25. Gao Y, Sun J, Lin W-H, Webb DJ, Li D. Microfluid. Nanofluid. 2011; 12:887–895. [PubMed: 22737106]
26. Buxboim A, Geron E, Alon R, Bar-Ziv R. Small. 2009; 5:1723–1726. [PubMed: 19415650]
27. Butler KL, Ambravaneswaran V, Agrawal N, Bilodeau M, Toner M, Tompkins RG, Fagan S, Irimia D. PLoS One. 2010; 5:e11921. [PubMed: 20689600]
28. Kim M, Kim T. Anal. Chem. 2010; 82:9401–9409. [PubMed: 20979359]
29. Zhu X, Si G, Deng N, Ouyang Q, Wu T, He Z, Jiang L, Luo C, Tu Y. Phys. Rev. Lett. 2012; 108:128101. [PubMed: 22540625]
30. Berthier E, Surfus J, Verbsky J, Huttenlocher A, Beebe D. Integr. Biol. 2010; 2:630–638.
31. Kim E, Schueller O, Sweetnam PM. Lab Chip. 2012; 12:2255–2264. [PubMed: 22437145]
32. Hancock MJ, He J, Mano JF, Khademhosseini A. Small. 2011; 7:892–901. [PubMed: 21374805]
33. Cho H, Hashimoto T, Wong E, Hori Y, Wood LB, Zhao L, Haigis KM, Hyman BT, Irimia D. Sci. Rep. 2013; 3:1–7.
34. Kim JY, Baek JY, Lee KA, Lee SH. Sens. Actuators, A. 2005; 119:593–598.
35. Devaraju NSGK, Unger MA. Lab Chip. 2012; 12:4809–4815. [PubMed: 23000861]

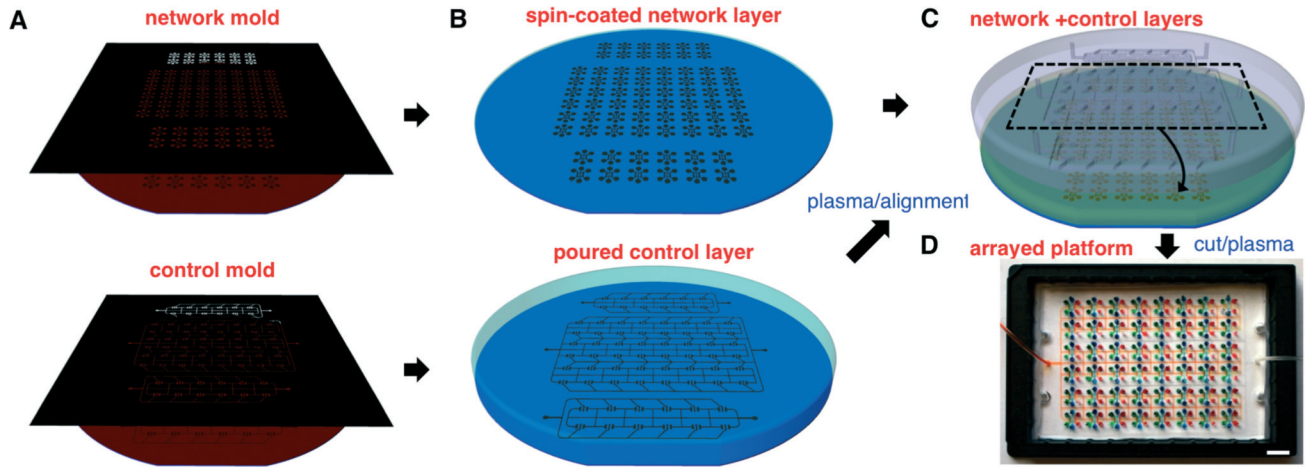

Fig. 1.

Wafer-scale fabrication of arrayed chemotaxis platform. A. Standard photolithographic techniques are used to fabricate SU-8 master molds on 6″ silicon wafers, for the network (upper) and control (lower) layers, respectively. B. PDMS-curing agent mixture is spun-coated and poured to create replicas of the network (upper) and control layers (lower), respectively. C. After curing, plasma-treated PDMS layers are aligned using ethanol as a lubricant and then dried to establish contact between the layers. D. Bonded layers of forty-eight platforms are cut and plasma-treated for bonding to a glass-bottomed plate as a single piece with two control lines for large-scale applications. Scale bar, 1 cm.

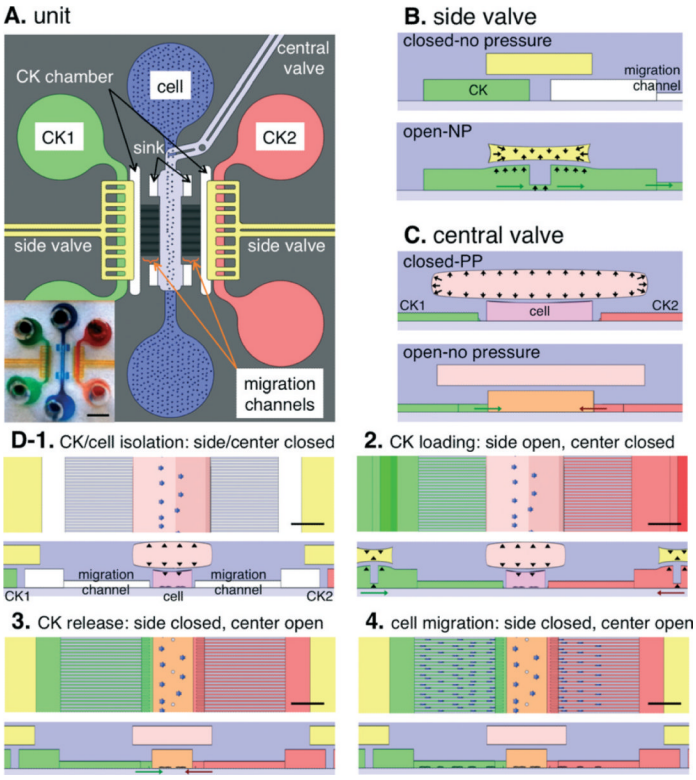

Fig. 2.

Schematic representations of on-demand and competing chemotaxis assay. A. Chemokines are loaded in both side compartments (CK1 and CK2) and cells are plated in a middle cellular compartment. These compartments are separated by two side valves (default-closed) and one central valve (default-open), respectively. Sinks between those compartments are designed to balance the difference in priming time of chemokine gradients caused by different diffusivity. Inset shows a photo of the platform visualized by food dyes. B. Two side valves are opened shortly to prime chemokine chambers and migration channels with chemokines and then closed to prevent any disturbing convection flow into the migration channels during chemotaxis assay. C. To plate the cells in the central compartment, the central valve is kept closed, sealing the compartments and avoiding early exposure to chemokines. To expose the cells to chemokine gradients and start the chemotaxis, the central valve is released without any pressure. D. The platform operates in two steps: chemokine priming and chemotaxis. (1–2) With opening of the side valves and closing of the central valve, chemokines fill the chemokine chambers and the migration channels. (3–4) With closing of the side valves and opening of the central valve, chemokines release and activate cell chemotaxis. Scale bars, 2 mm (A) and 200 μm (D).

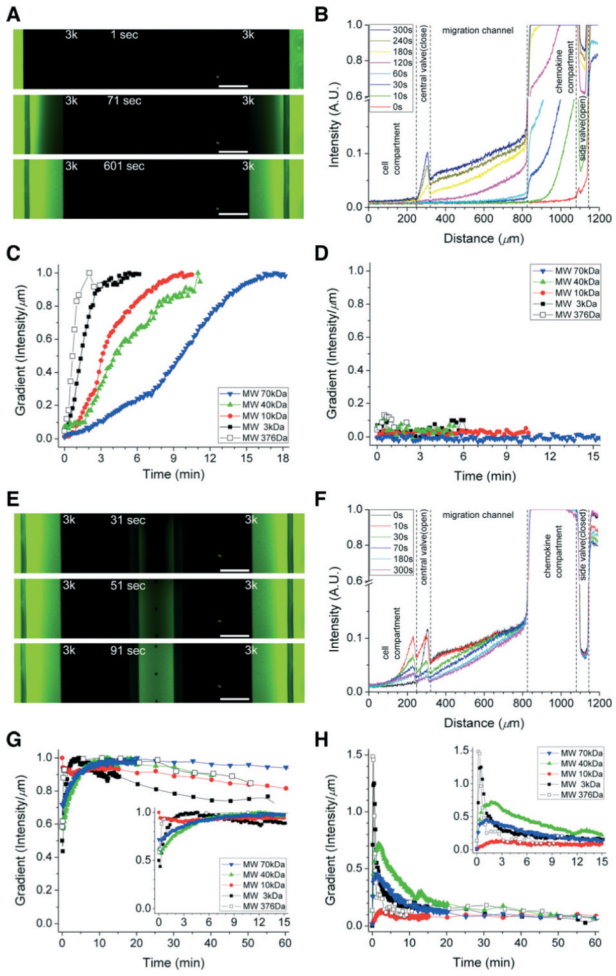

Fig. 3.

Validation of the initiation and stabilization of gradients for on-demand chemotaxis assay. A–B. Priming the devices and the formation of chemical gradients inside the devices was visualized using FITC-labelled dextran (MW 3 kDa). C. After opening the side valves, chemokine gradients along the migration channels are formed and stabilized within 2 to 15 minutes. Results are presented for fluorescein and various dextran-conjugated dyes, with various molecular weights, ranging from 376 to 70 000 Da. D. The central compartment remained chemokine-free during the priming period. E–F. The initiation of the chemokine gradients was visualized using FITC-labelled dextran (MW 3 kDa). G. After opening the central valve, chemokine gradients along the migration channels were formed and stabilized within 5 minutes. These gradients remained above 80% of the initial slope for over an hour. H. Chemokine gradients along the central compartment also stabilized within 10 minutes and were relatively stable for over an hour. Scale bars, 200 μm.

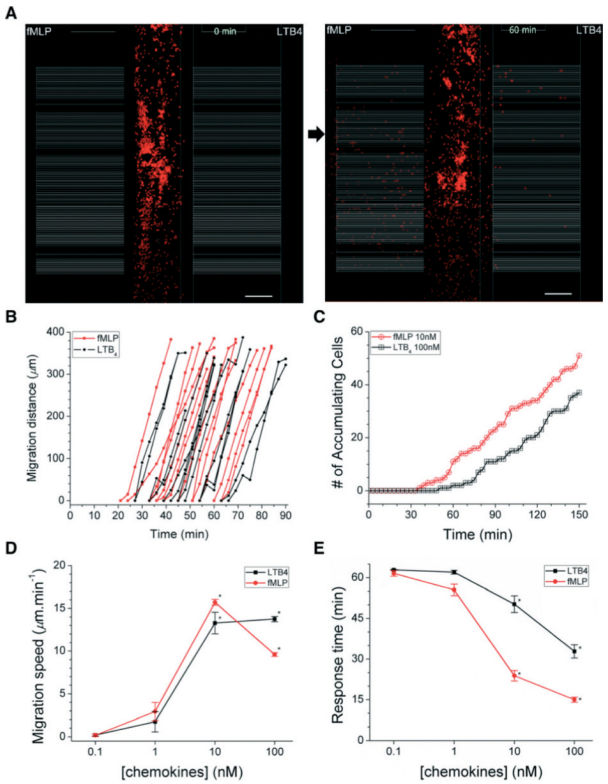

Fig. 4.

Dominant chemotactic response of human neutrophils to fMLP gradients. A. Individual neutrophils were tracked in fluorescent microscope (left panel: time 0 min, right panel: time 60 min) and their chemotactic activity is compared under dual gradients of fMLP at 100 nM and LTB_4 at 100 nM. B. No significant differences in migration speed exist between chemokines. C. Migration toward the fMLP chamber begins earlier than toward the LTB_4 chamber and consequently more neutrophils reach the fMLP chambers. D. Neutrophil chemotaxis shows the peak activity in migration speed at 10 nM of fMLP and between 10 to 100 nM of LTB_4. E. The neutrophil chemotaxis response time decreases with increasing concentrations of fMLP and LTB_4. On average, chemotaxis towards fMLP starts within 15 minutes at 100 nM, ~2 fold faster than towards LTB_4 at the same concentration. (Student's t-test. * $P < 0.0001$ with respect to no-chemokine condition). $n_{cell} = 318$ for migration speed and $n_{cell} = 61$ for response time at each concentration. Data represent mean ± s.e.m. Scale bars, 200 μm.

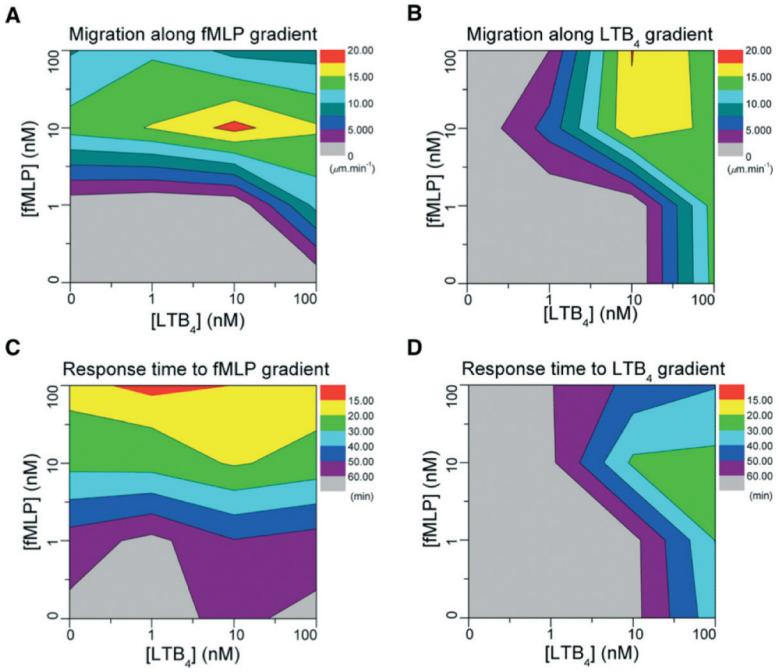

Fig. 5.

Chemotaxis speed and response time in the presence of simultaneous fMLP and LTB_4 gradients of various slopes. Contour maps of speed (A) and response time (C) show that chemotaxis towards fMLP is not affected by the presence of LTB_4. However, chemotaxis towards LTB_4 is affected by the presence of fMLP and the response is faster in the presence of fMLP, both in speed (B) and time (D). n_{cell} = 80 for migration speed and n_{cell} = 15 for response time at each combination of concentration. Data represents mean values (N = 3).